Different Cathode Architectures for Lithium-Selenium Batteries

A Project Report

Submitted to the Department of Chemistry

Indian Institute of Technology, Hyderabad

As part of the requirement for the of degree

MASTER OF SCIENCE

By

SNEHASIS BHUNIA

(Roll No. CY14MSCST11021)

Under the supervision of

Dr. M.Deepa

भारतीय प्रौद्योगिकी संस्थान हैदराबाद
Indian Institute of Technology Hyderabad

DEPARTMENT OF CHEMISTRY

INDIAN INSTITUTE OF TECHNOLOGY HYDERABAD

INDIA

APRIL 2016

Declaration

I hereby declare that the matter embodied in this report is the result of investigation carried out by me in the Department of Chemistry, Indian Institute of Technology Hyderabad under the supervision of **Dr. M.Deepa.**

In keeping with general practice of reporting scientific observations, due acknowledgement has been made wherever the work described is based on the findings of other investigators.

Snehasis Bhunia

(Signature)

Snehasis Bhunia

(Student Name)

CY14MSCST`11021

(Signature of Supervisor)

Dr. M. Deepa
Head & Associate Professor
Department of Chemistry
Indian Institute of Technology Hyderabad
Kandi-502285, Sangareddy, Telangana, India

Approval Sheet

This thesis entitled **"Different Cathode Architectures for Lithium-Selenium Batteries"** by Snehasis Bhunia has been approved for the degree of Master of Science from IIT Hyderabad.

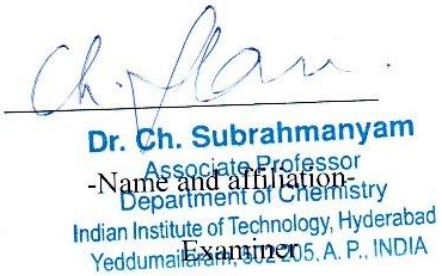

-Name and affiliation-

Examiner

Dr. S RENDRA K. MARTHA
Assistant Professor
D partment of Chemistry
Indian stitute of Technology Hyderabad

-Name and affiliation-

Examiner

-Name and affiliation-

Adviser

Dedicated to

My Beloved Parents

And

Respected Teachers

Contents

Acknowledgement

First, I would like to express my appreciation and heart-felt gratitude to my supervisor Dr. M.Deepa for his tremendous encouragement and guidance. I would like to thank him for encouraging my project work and helping me to do my project work. It was really a great honor for me to work under his guidance. Her advice on my career as well as on my project work has been priceless.

My warm thanks to IIT Hyderabad to provide instrumental facilities to the Department Of Chemistry at IIT Hyderabad.

I would like to thank PhD scholar M.Radha for his guidance. I am extremely grateful to other PhD scholars for their encouragement in learning experimental techniques and their helpful thoughts in my Project work.

My special thanks to my group members and my classmates. I would like to express my sincere thanks to Mr. S Krishna Kumar for her involvement in XRD spectra of my samples. I also cherish the sweet memories of all of my classmates, which I carry forward throughout my life. I am very much thankful to every research scholar in the Department of Chemistry, IIT Hyderabad who helped me to record the Spectroscopic data, for I have completed my project within the limited time.

Abstract

The Lithium-Sulfur battery has a high theoretical capacity (1675 mAh g^{-1}) and sulfur is highly abundant in earth crust and is inexpensive. But due to some serious issues like low conductivity (5 x 10^{-28} S m^{-1}), high rate of capacity fading due to polysulfide dissolution, long term cycling stability is not as good as that achieved in Lithium ion batteries. To alleviate some of these issues, the Lithium-Selenium battery was proposed. Although the theoretical gravimetric capacity (675 mAh $g^{-1)}$ is lower than sulfur for selenium, selenium has high conductivity (10^{-3} S m^{-1}), and has a comparable volumetric capacity with sulfur. However, selenium also exhibits the shuttle effect, and polyselenides dissolution in the electrolyte during cycling, which leads to capacity fade. To counter these issues, here, four types of selenium based active materials were prepared and evaluated for their ability to serve as cathodes in Li-Se cells. (1) A composite of commercial selenium and carbon black was prepared but it shows capacity fading and low conductivity. (2) A composite of Se with highly conductive multi walled carbon nanotubes (MWCNTs) was prepared; while cycling stability and coulombic efficiency are reasonably good but capacity is low. (3) A Se@GO (graphene oxide) composite was prepared by ball milling; it show very high capacity (650mAh g^{-1}) but due to low conjugation in GO, its cycling stability is not good. (4) A Se@RGO (reduced GO) composite was prepared by an in-situ hydrothermal method; RGO has higher conjugation and GO like structure, capacity fading was not as severe as in the previous composites and its' coulombic efficiency is good. These preliminary studies show the promise which Se@carbon nanostructures composites have for stable Li-Se cells.

Introduction

1. Introduction

According to an energy outlook 2014 by U.S Energy Information Administration, the global supply of crude oil, coal, liquid hydrocarbon etc. can meet the world's energy demand up to 25 years. So energy challenge faced by world mainly depends upon two factors.

1. Production of electricity from non-renewable source to renewable sources.
2. All the vehicle companies moving towards electrical propulsion, mainly due to the rise of environment issues and petrol price.

The sources of sustainable energy are fluctuating day by day and sustainable energy use requires the perfect way to store energy like battery. Recently, sustainable energy source research have been developed by better wind mills, turbines, photo thermal receivers, solar cells[1], but energy storage research is continuously evolving. The development of a battery which can store high energy, has good stability, high cycling stability, and is also environment friendly, is a major challenge in electrochemical research.

In this context, the lithium ion battery, which has moderate energy density and very good cycling stability is an attractive solution. The year 1980 was a very important year for electrochemical research. Two major discoveries were made first one is lithium cobalt oxide for cathode material, by American chemist John B. Goodenough, and second one is graphite for anode material by Rachid Yazami from Morocco. With these discoveries, the Japanese scientist Akira Yoshino at Asahi Chemical built the lithium ion battery in the year 1985, which was commercialized in 1991 by Sony-corporation.

Mainly lithium ion battery works by following way.

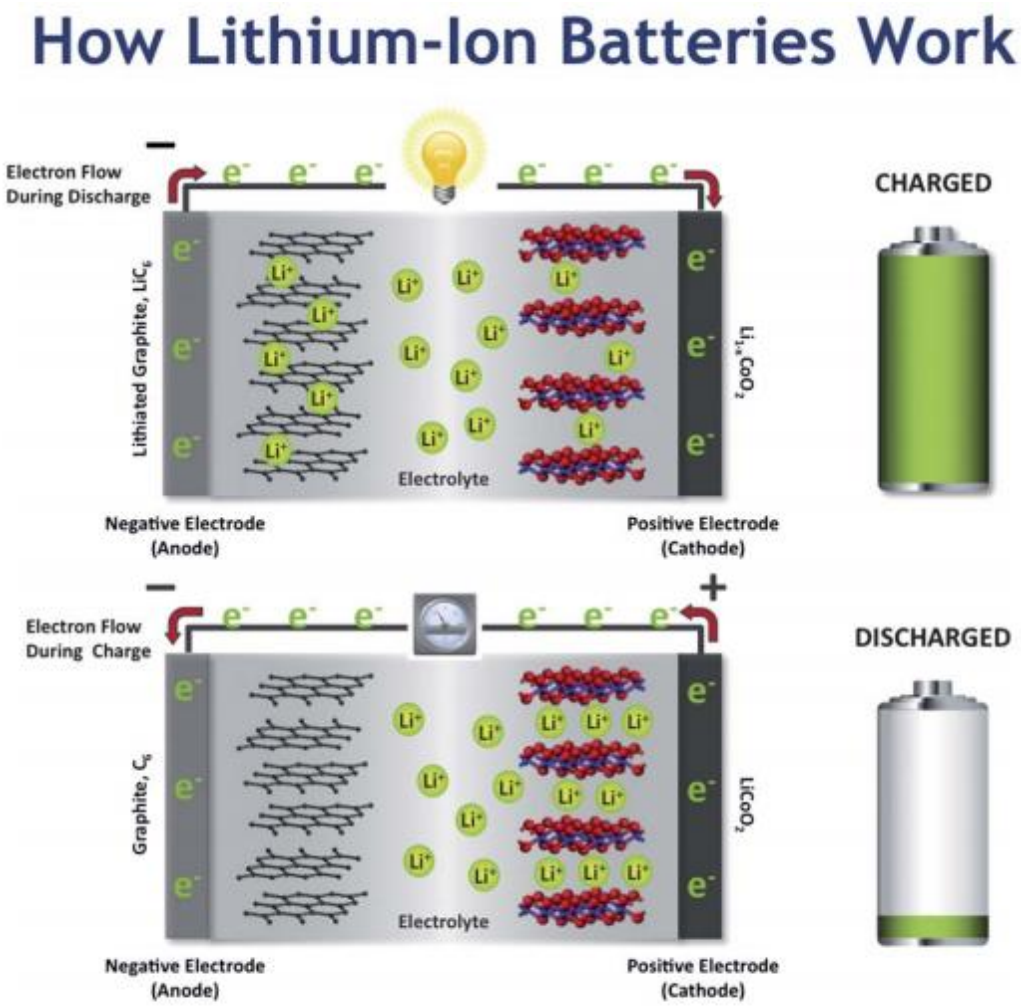

Fig 1- Working principle of lithium ion battery (Copyright 2011 ACS Publishers Ltd.)

At the time of charging, the lithium ion moves from cathode side to anode side and electron moves through external circuit. Then lithium ion intercalates into the graphite layer. The reactions are -

At cathode- $LiCoO_2 \rightarrow 0.5\ Li + 0.5\ e^- + Li_{0.5}CoO_2$

At anode - $C_6 + Li^+ + e^- \rightarrow LiC_6$

For Lithium cobalt oxide, upper potential for delithiation is 4.2 V. So for the transformation from $LiCoO_2$ to $Li_{0.5}CoO_2$ the capacity will be half of the theoretical capacity, which is about 140 mAh/g. Here lithium source is lithium cobalt oxide, which is extremely stable and follows all safety features. But there are some drawbacks in lithium cobalt oxide such as high cost, toxicity, chemical instability at the time of deep charge that's why it is used only in portable

electric devices, not in transportation and stationary storage applications. There are another two cathode materials which are cheaper and follow the safety features. They are the spinel $LiMn_2O_4$ and the Olivine like structure $LiFePO_4$, they are environment- friendly, have good structural and chemical stability and also have a high charge-discharge rate capability. In $LiMn_2O_4$ there is a major problem. It has limited energy and Mn dissolution occurs when disproportion reaction occurs from Mn^{3+} to Mn^{2+} and Mn^{4+}. This has been solved by introducing lower valent cation like Li^+ and Ni^+ in $LiMn_2O_4$. This increases the average oxidation sate of Mn from 3.5+ to 3.6+ and as a result, Mn dissolution and dynamic Jahn-Teller distortion are suppressed, and performances are also increased. Often to increase more performance, the spinel cathode is mixed with 30% wt of layered oxide ($LiNi_{1/3}Mn_{1/3}Co_{1/3}O_2$) and this increases the capacity and reduces further Mn- dissolution. On the other hand, $LiFePO_4$ has a big role in vehicle applications. But there also some issues such as there is poor lithium conduction and electrical conductivity. This is solved by making it nano-sized and by using conductive carbon at the time of cathode preparation. Graphite is used as an anode in Lithium ion battery. The table below provides a summary of all electrode materials.

Table-2:

Electrode Materials	Cell voltage	Capacity	Specific Energy	Advantages
Layered $LiCoO_2$ cathode(2d-structure)	4	140	560	High electronic and Li^+ conductivity; revolutionized the portable electronic market
Spinel $LiMn_2O_4$ cathode(3d-structure)	4	120	480	Inexpensive and environmentally benign Mn; high electronic and Li^+ conductivity; excellent rate capacity, good safety
Olivine $LiFePO_4$ cathode(1d-structure)	3.5	160	560	Inexpensive and environmentally benign Fe; covalently bonded PO_4 groups lead to excellent safety
Graphite anode	1	370	-	Inexpensive and environmentally benign C; low operating potential maximizes cell voltage

Fig. 2- Various cathode materials used in LIBs.

At the graphite, electrode lithium insertion occurs by first order phase transition performing various stages, and forms LiC_x (where x=24, 27, 12) when the graphite electrode is kept in lithium salt first it consumes some charge irreversibly to reduce the solution species, then form a film which is called Solid Electrolyte Interface (SEI). By this layer lithium ion is permissible and it forms one time only. During lithium ion insertion this SEI layer prevents any further irreversible process and creates a metastable state for highly reducing Li_xC [3].

The choice of electrolyte solution is an important matter. Mostly, reserachers use alkyl carbonates for best performance[4]. Binary mixtures are used are used, such as ethylene carbonate (EC) and dimethyl carbonate (DMC) or ethyl methyl carbonate (EMC) and diethyl carbonate (DEC) propylene carbonate (PC). The structures of solvents are shown below.

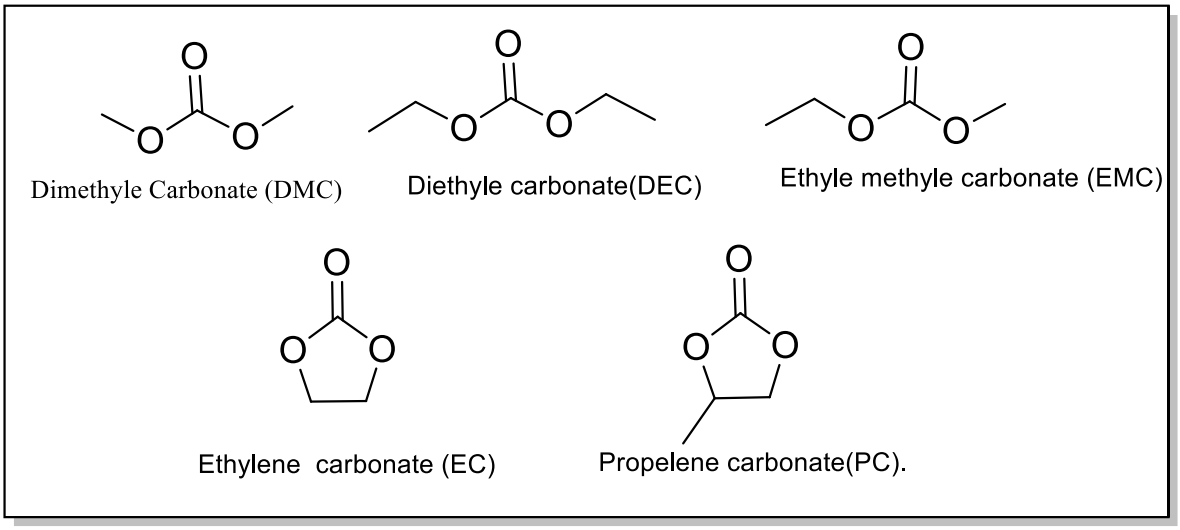

Fig.3 Solvents used in lithium based batteries

The lithium salt that is used in most of the cases is $LiPF_6$. When potentiodynamic test is done in an inert electrolyte in non-aqueous polar aprotic solvent with tetra alkyl salt then the following curve is obtained.

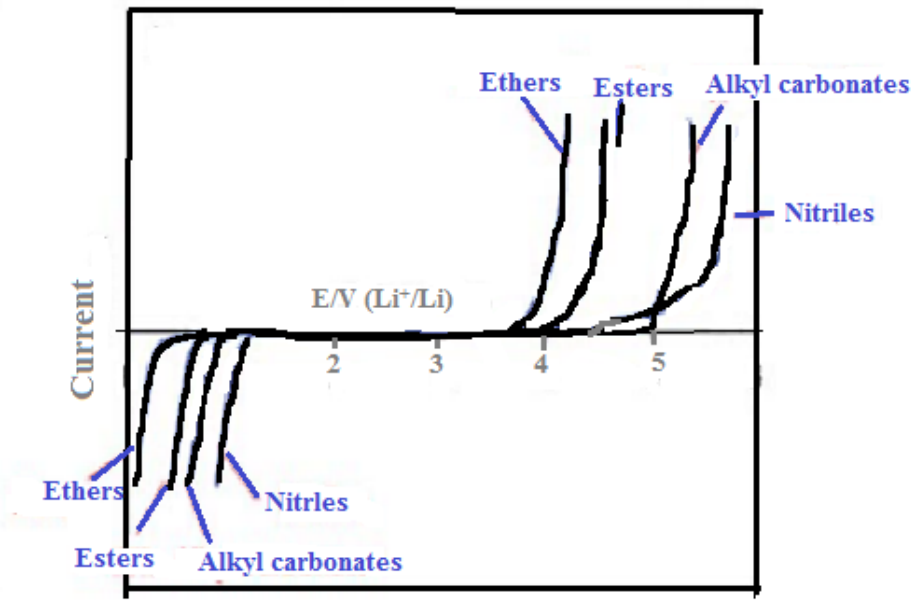

Fig.4 Potentio-dynamic diagrams for electrolyte solutions

It is shown that the solvent molecules, which contain more atoms with higher oxidation state, will be more anodically stable[6]. When lithium ion remains in the non-aqueous solution then reduction process occurs in complete different ways with respect to tetra alkyl salts. The trace

amounts of O_2, H_2O, salt anions solvent (ethers, esters, and carbonates) are reduced and forms insoluble compounds to mother solution. All the reduced products are listed in the following table.

Solution Species	**Main reduction products (not all)**	**Potential range vs. Li/Li+**
O_2	LiO_2^-, Li_2O_2	1.5–2 V
H_2O	LiOH	1.5–1.2 V
HF, PF_5	LiF, Li_xPF_y	1.8 V and below
Ethers	ROLi	Below 0.5 V
Esters	$ROCO_2Li$ (carboxylates)	Below 1.2 V
Alkyl carbonates	$ROCO_2Li$, ROLi	Below 1.5 V
EC	$(CH_2OCO_2Li)_2$, C_2H_4	Below 1.5 V
PC	$CH_3CH(OCO_2Li)$ CH_2OCO_2Li	Below 0.5 V
DMC	CH_3OCO_2Li,CH_3OLi	Below 1.2 V
$LiClO_4$	LiCl,$LiClO_x$	Below 1 V
$LiPF_6$	LiF, Li_xPF_y	Below1 V
LiN	LiF, $LiCF_3$, $LiSO_2CF_3$ $Li_2NSO_2CF_3$	Below 1 V
$(SO_2CF_3)_2$		Below 0.5 V

Fig.5 Reduced products of solvents in LIBs.

They all precipitate on the lithium metal or graphite. This can be explained by the following diagram.

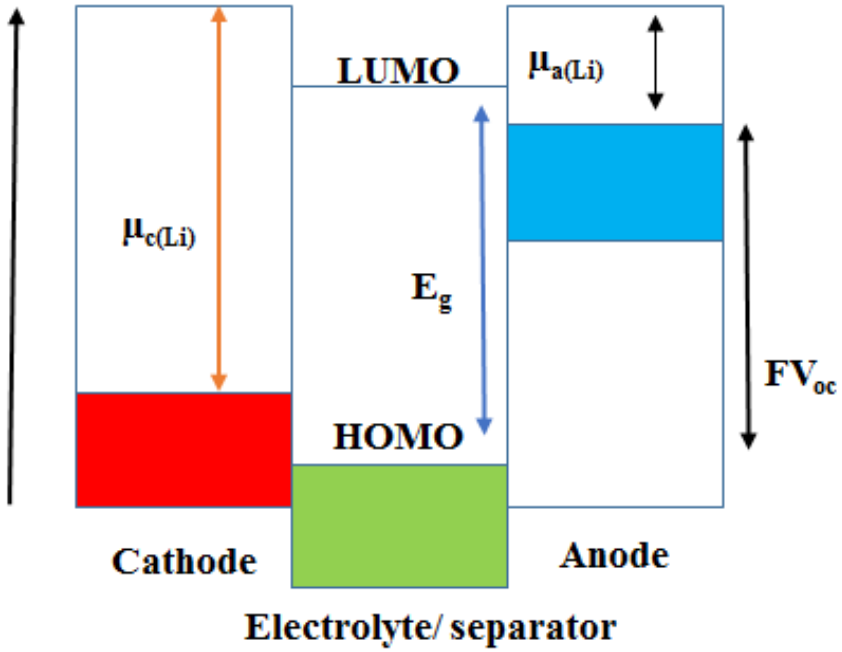

Fig.6- Schematic energy diagram of a lithium cell at open circuit.

After reaching certain thickness, they stop further electron flow. This thin layer is called SEI layer. SEI, by creating a barrier between electrolyte and anode stops further reduction and increases stability. So the selection of electrolyte is very much important for anodic stability of electrolyte solution. So previously discussed EC-DMC and $LiPF_6$ are most preferred electrolyte solutions for lithium ion batteries, and there are some extra reasons also[6].

1. EC-DMC/ $LiPF_6$ shows high electrical conductivity at high and low temperature (up-to -15 ^oC).
2. In EC-DMC the central carbon is oxidized to its highest oxidation state (IV) and it has relatively lower number of C-H bonds which are considered as electron donating nobilities. For these reasons its anodic stability is highest.
3. Carbonates have 3 oxygen which coordinates Lithium ion very well. So solubility of $LiPF_6$ in EC-DMC is very high.

Now we will discuss about advantages and disadvantages of lithium ion battery. We know energy density of a battery depends proportionally upon voltage and specific capacity, but

researchers are using high voltage and high capacity materials. Some well-known cathode materials are olivine $LiCoPO_4$, $LiNiPO_4$, spinel $LiMn_{1.5}Ni_{0.5}O_5$, they have operating voltages of, respectively, 4.8, and 5.2, 4.7 V. On the other hand there are high capacity cathode materials, such as lithium rich layered $Li[Li,Mn,Co]O_2$ and $LiMSiO_4$ (M= Fe, Co, Ni). Main drawbacks of these materials are that at high voltage, the electrolytes are very unstable, they decompose at high voltages. If the main aim is to introduce a battery with high energy density then the following voltage vs capacity plot is relevant, and Sulfur and oxygen as cathode materials in Li-S and Li-air batteries were employed.

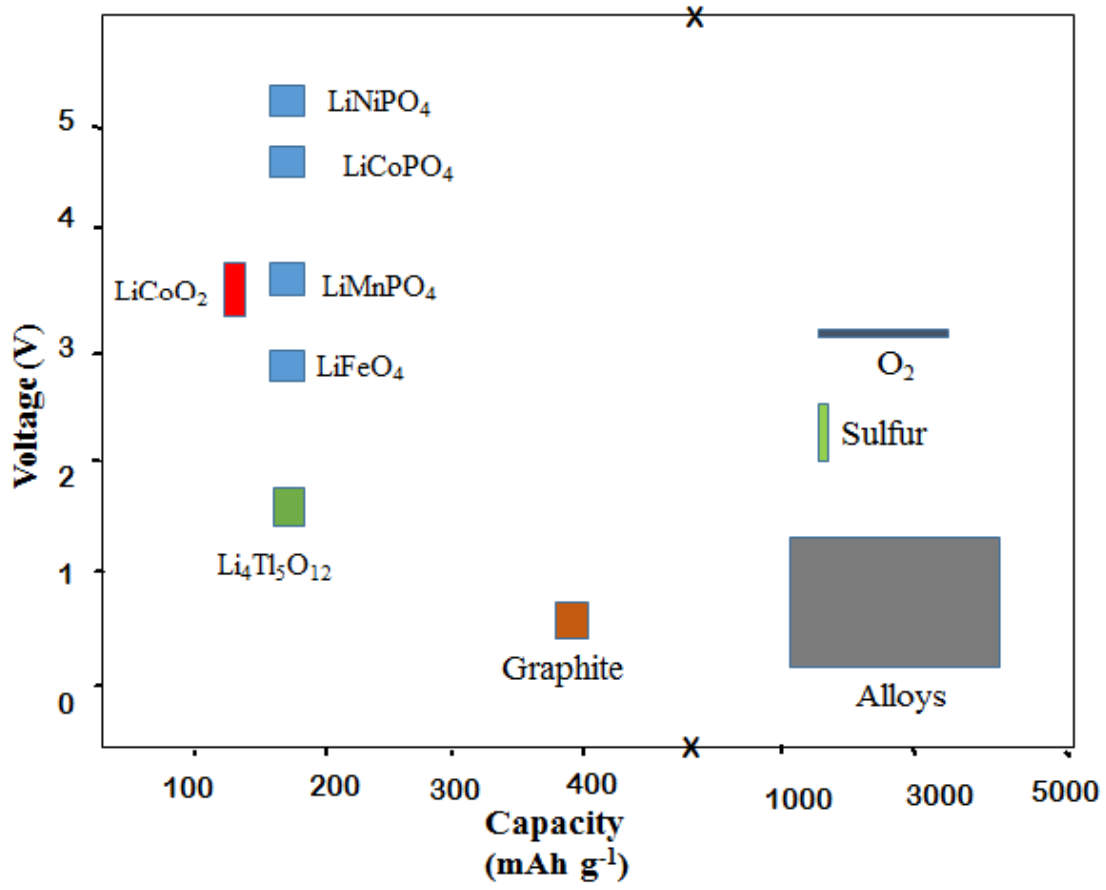

Fig.7- Voltage vs Capacity plot for various cathode materials.

Sulfur was used as a cathode material in storage batteries by Herbet and Ulam in 1962. Later on, Rao specifically patented high-energy-density metal−sulfur batteries with organic electrolytes and presented the theoretical energy densities of metal−sulfur cells in 1966[7]. Sulfur is one of the most abundant material on the earth crust having a high theoretical capacity of 1672 mAh/g and this is a very high capacity with respect to transition metal oxide cathodes. A lithium sulfur cell is a storage device which stores electrochemical energy at the sulfur cathode. The following diagram shows the working principle of a lithium sulfur battery.

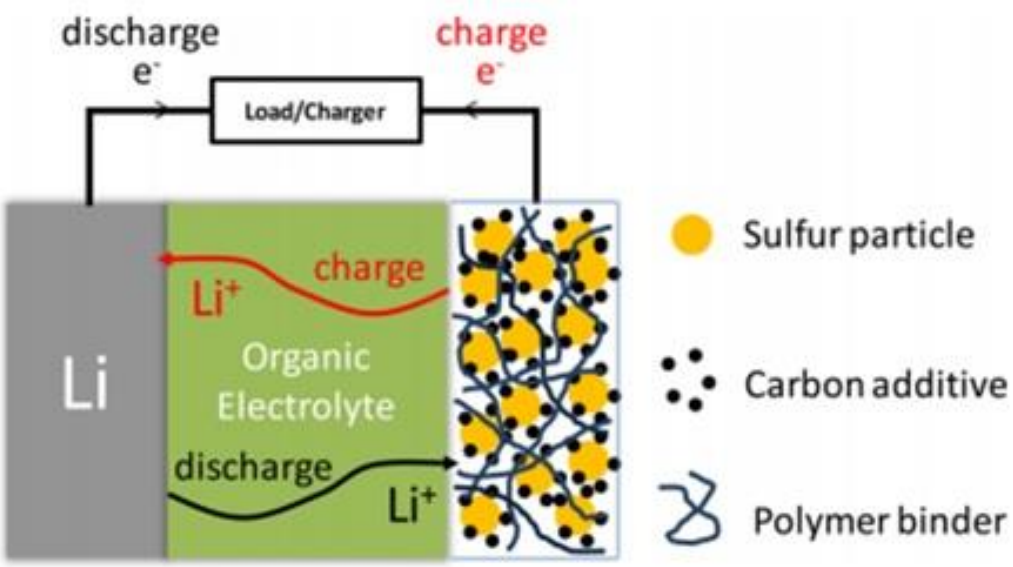

Fig 8- Charge-discharge diagram for lithium sulfur/selenium battery (Copyright 2009 ACS Publishers Ltd.)

A conventional lithium sulfur battery consists of Li metal as an anode, organic electrolytes and a sulfur composite as a cathode. Since sulfur is in the charged state, the battery starts working with discharge first. During discharge, lithium metal becomes oxidized and make the electrode negatively charged, and forms lithium ion and electron. Lithium ion moves from the cathode side to the anode side through the electrolyte solution and electron flows from cathode to anode via the external circuit. This electron reduces the sulfur cathode and makes it lithium sulfide

by taking that lithium ion. The reactions occurring during discharge are given below, and the backward reactions will occur during charge[8].

- **Negative electrode**: anodic reaction (oxidation) : $2Li \rightarrow Li^+ + 2e^-$
- **Positive electrode**: cathodic reaction (reduction) : $S + Li^+ + 2e \rightarrow Li_2S$
- **Over all cell reaction** (discharge) : $2Li + S \rightarrow Li_2S$

The theoretical capacities for lithium and sulfur are 3.861 and 1.672 Ah/g, respectively, and overall theoretical cell capacity is 1.167 Ah/g for the Li−S cell. The discharge reaction has an average cell voltage of 2.15 V. Hence, the theoretical gravimetric energy density for a Li-S cell is 2.51 Wh/g.

There is a strong tendency of sulfur to make sulfur-sulfur bond due to catenation property. It forms long homo atomic chain or homo-cyclic rings of various sizes. Octa-sulfur (cyclo-S_8), crystallizing at 25 °C as orthorhombic α-S_8, is the most stable allotrope at room temperature. At the time of discharge, the first S_8 ring is opened by reduction and forms higher order lithium poly-sulfides, Li_2S_x ($6<x\leq8$). As the discharge continues, lower order poly-sulfides Li_2S_x ($2<x\leq6$) are formed with incorporation of additional lithium. The reduction occurs at two different voltages, at 2.3 V, S_8 forms Li_2S_8 and Li_2S_6 and at 2.1 V, Li_2S_4, Li_2S_2, Li_2S are formed. These are shown in the following figure.

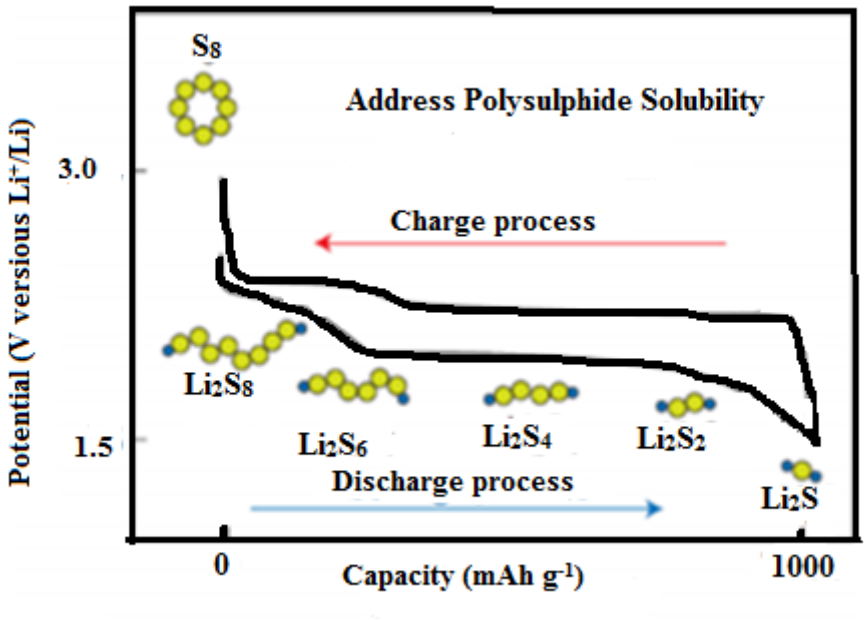

Fig. 9- Voltage profile for lithium sulfur cell.

At the time of charging, Li_2S converts to S_8 via formation of intermediate lithium polysulfides. This charge discharge process forms a reversible cycle. However, the two charge voltage plateaus are normally overlapped with each other.

There are many technical challenges in Li-S technology, either with the system or with the material[9].

- **Resistance:** First of all, sulfur has a very high resistance, it implies very low electrochemical conductivity ($\sim 10^{-30}$ S/cm). To increase conductivity, lot of conductive carbon is added; almost 10-15% of cathode weight.
- **Shuttle effect**: During cycling, the intermediate poly-sulfides (Li_2S_x) are formed, there are formidable changes in their structure and morphology. That's why they are not attached with current collectors. They dissolve in the electrolyte solution. This is accompanied by loss of active mass of cathode. So overall capacity decreases.[10]
- **Self-discharge**: Like nickel-cadmium and Nickel metal hydride battery, the Li-S battery has also some self-discharge property. At the resting stage, sulfur dissolves in the electrolyte and moves to the anode side through separator due to concentration difference.

That sulfur reacts with lithium and makes poly-sulfides. So open circuit voltage (OCV) and overall capacity decreases[11].

These issues result in a low utilization of the active material, poor cycle life, and low system efficiency. Thus, the conventional Li-S battery electrode shown in cannot meet all the requirements of Li-S batteries for practical applications. Selenium, as a congener of sulfur in periodic table has similar chemical properties. There are some advantages of selenium:

- The electronic conductivity of selenium (1×10^{-3} S/m) is more than that of sulfur (5×10^{-28} S/m), and a recent result showed that lithiated selenium (Li_2Se) might be more conductive than lithiated sulfur (Li_2S); it indicates that selenium will show higher electrochemical activity than sulfur.[12]
- Although the gravimetric capacity of selenium (678 mAh/g) is lower than the sulfur (1650 mAh/g) but the volumetric capacity of selenium (3253 Ah/L) is comparable to that of sulfur (3467 Ah/L) because the density of selenium is 2.5 times higher than that of sulfur. Generally, the volumetric capacity is important when battery is used for portable devices or electric vehicles, because battery should be packed in a limited space.[12]
- Polyselenides dissolution is lower than polysulfide dissolution. So loss of active material is lower than sulfur[12].

Although on the basis of these advantages, selenium is getting popular as a cathode material, but there are some disadvantages like dissolution of higher order polyselenides, which leads to loss of active mass of cathode and as a result, capacity fading (shuttle effect). To overcome these problems, efforts have been devoted to encapsulating selenium into porous carbons, graphene materials, or conductive polymers to trap the polyselenides. In our work, we added a carbon coated barrier layer and performance is improved.

Experimental section

2.1 Preparation of Selenium nanoparticles

0.4 gm of SeO_2 (Alfa Aesar) was dissolved in 20 ml of deionized water, and stirred for 15 min, after stirring well, 1 ml TWEEN-20 (Polysorbate 20, Sigma-Aldrich) was added as a surfactant, and stirred for 10 minutes. At the stirring condition, 0.5 ml of N_2H_4 was added. The whole solution turned red and it was stirred upto 15 minutes. Then the whole solution was transferred into an autoclave. The autoclave was heated at 90 ˚C for 2 hours. Then the precipitate was collected and washed with alcohol for several times. It was dried in a vacuum oven for 6 hours at 60 ˚C. Then it was collected and stored.

2.2 Preparation of Se@RGO

First the GO was prepared by modified Hummers method[13, 14]. First 1g of graphite was dissolved in 24 ml of concentrated sulfuric acid. The mixture was stirred well in an ice bath for 4 hours. Then 3 ml of freshly prepared $KMnO_4$ was added slowly for 1 hour. The mixture was stirred well for 24 hours. The whole solution was poured into 30 ml of deionized water having 0.6 ml of H_2O_2. Then it was washed several times with water. Then the solution was centrifuged, wet graphene oxide was collected and dried for 12 hours.

- Selenium dioxide 0.4 g was dissolved in 20 ml of water and stirred well; then 0.5 g of GO was added and mixed by stirring. To the whole solution, 0.5 ml of $N_2H_4.H_2O$ was added. Then the solution was transferred into an autoclave (50ml) and heated at 90 ˚C for 2 h. Then it was washed with water and dried for 6 hours.

2.3 Preparation of Se@MWCNTs composite

0.5 g of commercial selenium and 0.5 g of MWCNTs (Sigma-Aldrich) were mixed well in mortar and pestle. Then it was heated at 260 ◦C for 12 hours in an argon atmosphere, and cooled to room temperature and collected it in sample vial.

2.4 Preparation of Se@GO composite

Commercial selenium and Graphene oxide were mixed in same amounts by weight (1:1) and mixed well in mortar and pestle for 1 hour. Then it was ball milled for 12 hours, and collected and stored.

2.5 Characterization

All the synthesized samples were characterized by using the following instruments.

- Field-emission scanning electron microscopy (SEM- FESEM, Carl Zeiss supra 40)
- X-ray diffraction technique (XRD- PANalytical X'pert PRO, with a Cu K_α radiation by applying an accelerating voltage 40kV and 30 MA current) in the range of 10-90◦ (2 theta).

2.6 Electrochemical measurements

Six type electrochemical measurements were done on the basis of different material and different percentage. They are as follows:

2.6.1 Cathode of Commercial selenium

The cathode material slurry was prepared by mixing of 80 wt. % of Commercial Selenium, 10wt. % carbon black, 10% wt. of Sodium alginate as a binder and NMP (N-Methyl-2-pyrrolidone) was used as a solvant.The slurry was coated on a stainless steel current collector, and diameter of 1 cm. active mass loading on current collector was 1.5-1.9 mg/cm^2. Then the discs were dried in vacuum oven at 60◦C. The Swagelok sell were assembled in the globe box filled with inert argon gas. At time of cell fabrication the oxygen

and water level was below the 1ppm. For the both case basic electrolyte was used 1 M LiTFSI in a solvent mixture of DME and DOL (1:1, v/v) .Lithium metal was used as counter electrode and standard size Celgard separator was used. Galvano static charge/discharge tests were performed in the voltage range of 0.8V to 3.0V at 25°C by using Arbin battery-testing instrument. The cells were first discharged to 0.8V and then the cycle number was counted. All the electrochemical tests were conducted at room temperature.

2.6.2 Cathode made up of Se@MWCNTs composite

Here cathode slurry was prepared by using a Se@MWCNT composite, conductive carbon black, and sodium alginate (binder) at 8:1:1 ratio. They were mixed very well in mortar and pestle. Water was used to make a slurry. It was applied on current collectors made-up of stainless steel, heated at 60°C in vacuum oven for 6 hours. The cathode was used in a Swagelok cell in an argon filled globe box at levels of less than 1ppm of oxygen and water. Lithium metal was used as a counter electrode. 1 M LiTFSI in a solvent mixture of DME and DOL (1:1, v/v) was used as an electrolyte and Li metal foil as an anode. Galvanostatic charge/discharge tests were performed in the voltage range of 0.8 V to 3.0 V at 25 °C by using Arbin battery-testing instrument. The cells were first discharged to 0. 8V and then the cycle number versus capacity were recorded. All the electrochemical tests were conducted at room temperature.

2.6.3 Cathode by using Selenium@GO composite

Ball milled selenium-graphene oxide composite, carbon black, sodium alginate was mixed in a 8:1:1 weight ratio. They were mixed well with water to make it into a slurry. The slurry was coated on a stainless steel current collector, radius of 1 cm. Active mass loading on current collector was 1.5-1.9 mg/cm^2. Then the discs were dried in a vacuum oven at 60 °C.

The Swagelok sell were assembled in the glove box filled with inert argon gas. At time of cell fabrication, the oxygen and water levels were below 1 ppm. For both cases, an electrolyte: 1 M LiTFSI in a solvent mixture of DME and DOL (1:1, v/v) was used, Lithium metal was used as a counter electrode and standard size cell Gard separator was used. Galvanostatic charge/discharge tests were performed in the voltage range of 0.8 V to 3.0 V at 25 ◦C by using an Arbin battery-testing instrument. The cells were first discharged to 0.8 V and then the cycling stability was examined. All the electrochemical tests were conducted at room temperature.

2.6.4 Cathode made up of Se@RGO

The synthesized Se@RGO was used at 80 wt. % and carbon black and sodium algenate binder were used at 10 wt. % each. Two drops of water was used to make aslurry. It was coated on a current collector and made dry by heating in a vacuum oven 60 ◦C for 6 hours. The Swagelok sell were assembled in the glove box filled with inert argon gas. At time of cell fabrication, the oxygen and water levels were below 1 ppm. For both cases, an electrolyte: 1 M LiTFSI in a solvent mixture of DME and DOL (1:1, v/v) was used, Lithium metal was used as a counter electrode and standard size cell Gard separator was used. Galvanostatic charge/discharge tests were performed in the voltage range of 0.8 V to 3.0 V at 25 ◦C by using an Arbin battery-testing instrument. The cells were first discharged to 0.8 V and then the cycling stability was examined. All the electrochemical tests were conducted at room temperature.

Results and Discussion

Five types of Se based materials were examined as cathodes for Li-Se batteries. Among them, the first two are the materials with commercial selenium. In both cases, there were two different percentages of Selenium and carbon black. These were used to compare the performances of elemental selenium a different proportions. We prepared the Commercial Selenium cathode by mixing with carbon black. It was characterized by field-emission scanning electron microscopy (FESEM, Carl Zeiss supra 40). The following figures 10a and 10b are the images of commercial selenium samples.

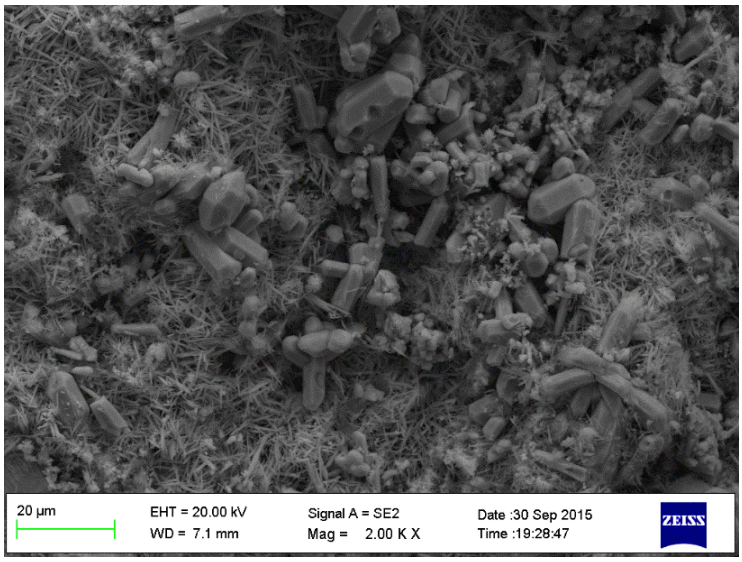

Fig- 10a

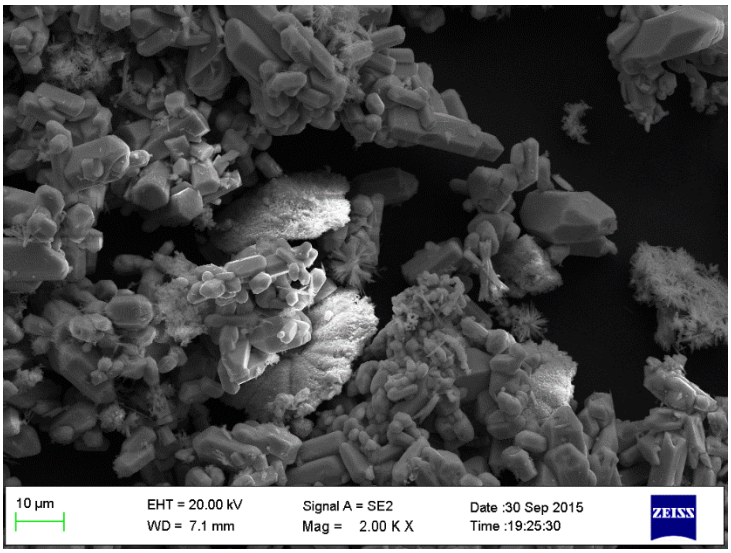

Fig- 10b

Fig.-10a and 10b- SEM images of commercial Selenium

It is clearly seen that commercial Se has rhombohedral shapes. At first, commercial selenium, carbon black and sodium alginate was taken with 8:1:1 ratio, and used in cells. The charge discharge was done in the voltage range of 0.8-3.5 V, where the OCV was 3.06 V. The high voltage is due to higher conductivity ($1x10^{-3}$ of selenium particles) and also due to the addition of highly conducting carbon black. The charge-discharge behavior of this cathode material is shown below in the figures 11a and 11b.

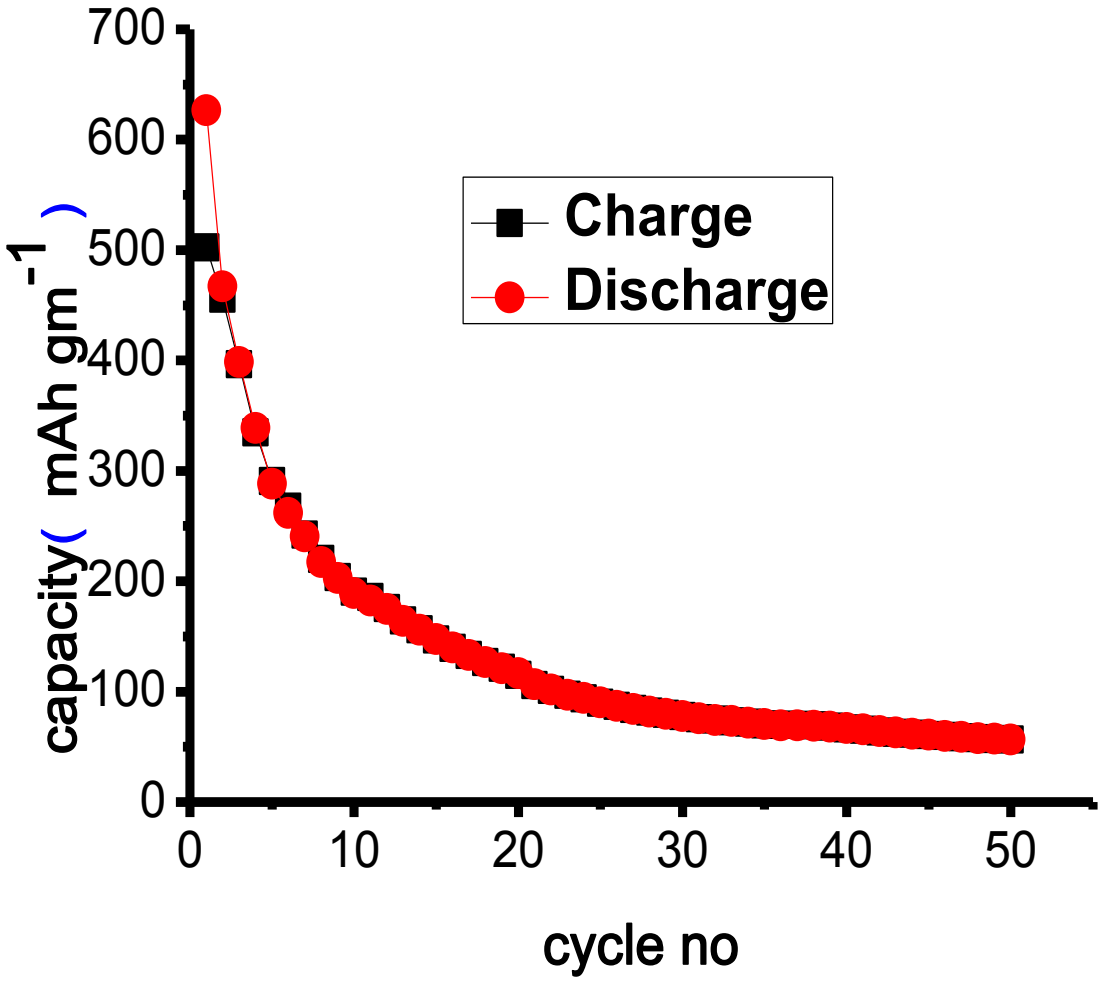

Fig.11a- Charge discharge capacity retention plot of Commercial Selenium cathode

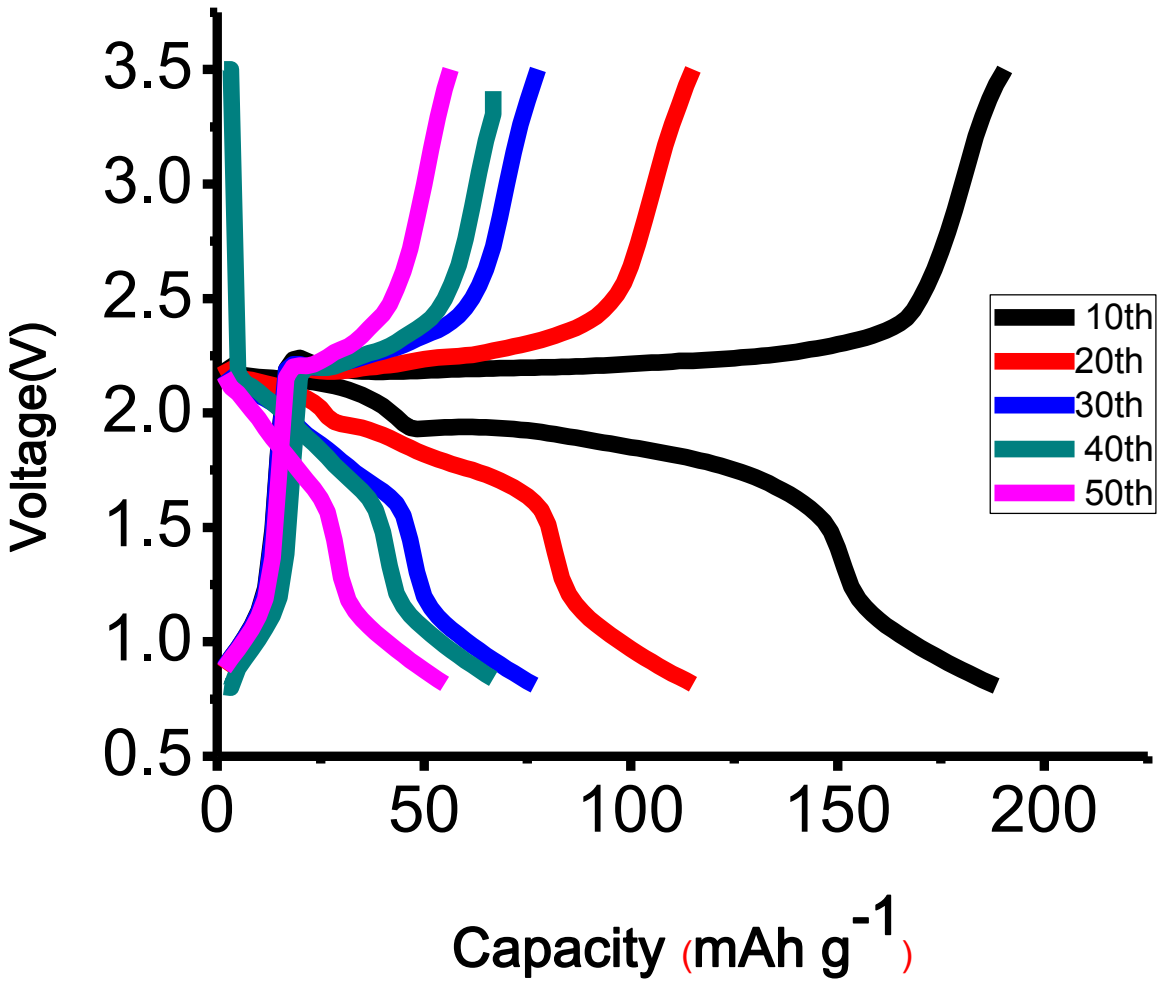

Fig.11b- Galvanostatic discharging-charging profile of the commercial Se cathodes at C/6.75 rate.

Initially, we see a very high capacity near 640 mAh g^{-1} and rapid capacity fading up-to 30th cycle. At the 30th cycle, the capacity is 95 mAh g^{-1}. Then cycling stability is good and it continues up-to 50th cycle. The side reaction between $LiSe_x$ and the carbonate electrolyte are main cause of the low capacity. In liquid electrolyte which has higher solubility for polyselenides than conventional carbonate electrolyte ($LiPF_6$ in EC/DEC) is employed for the Se cathode. The Se-carbon black cathode shows two plateaus at 2.2 and 1.8 V (shown in Figure 11b). The two plateau reaction was also observed for Se-Carbon cycling with LiTFSI in DOL/DME electrolyte by Cui et al[15]. The lithiation plateau at a high potential of 2.2 V is due

to the reduction of Se cathode to the soluble polyselenides, Li_2Se_x (x= 4), while the plateau at a low voltage of 1.8 V is due to further reduction of soluble Li_2Se_x (n= 4), to non-soluble Li_2Se_2, and Li_2Se[16]. During the delithiation process, Li_2Se is oxidized to Se_n^{2-} (n= 4) first, and then the high-order poly-selenide is further oxidized to Se. However, the high solubility of polyselenides in the LiTFSI-DME/DOL electrolyte also causes severe shuttle reaction, as evidenced by the voltage plateau at 2.2 V [17]. Since the mesoporous carbon material host can reduce from the side reaction between $LiSe_x$ and carbonate electrolyte and the stable Se-O layer is also formed on cathode surface can protect $LiSe_x$ for shuttling. So a Se-porous carbon composite as a cathode material was prepared. A Se@MWCNTs composite was prepared by first mixing of commercial Selenium and then heated at 260 ˚C in a tubular furnace in an argon gas atmosphere for 12 h. At the 260 ˚C, Se will be in molten condition and will be mixed well. The following SEM images show the structure of MWCNTs and Se@MWCNTs.

Fig. 12a- SEM image of MWCNTs.

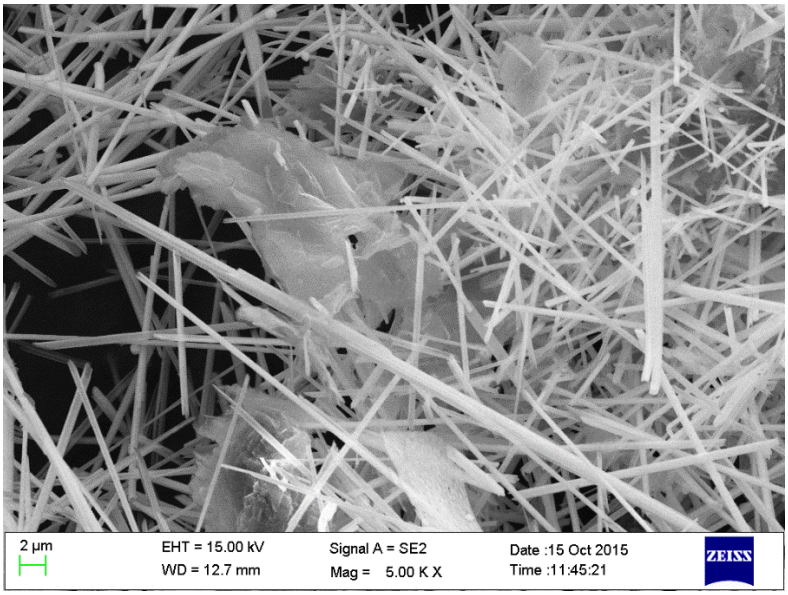

Fig. 12b- SEM image of Se@MWCNTs.

In the SEM image of pristine MWCNTs, the tubular structures of MWCNTs are observed. It is clearly seen that the mixing of MWCNTs and Se is inhomogeneous in the Se@MWCNTs composite, as particles of Se are segregated and so are the CNTs. The galvanostatic charge-discharge results are shown in Figures 13a and b.

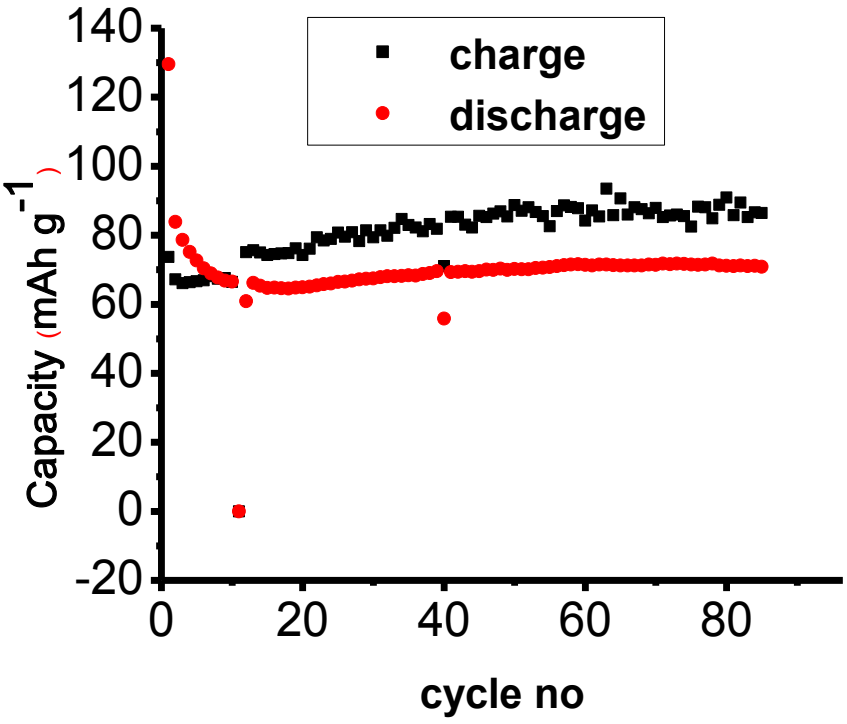

Fig. 13a- Charge discharge capacity retention plot of the Se@MWCNTs cathode.

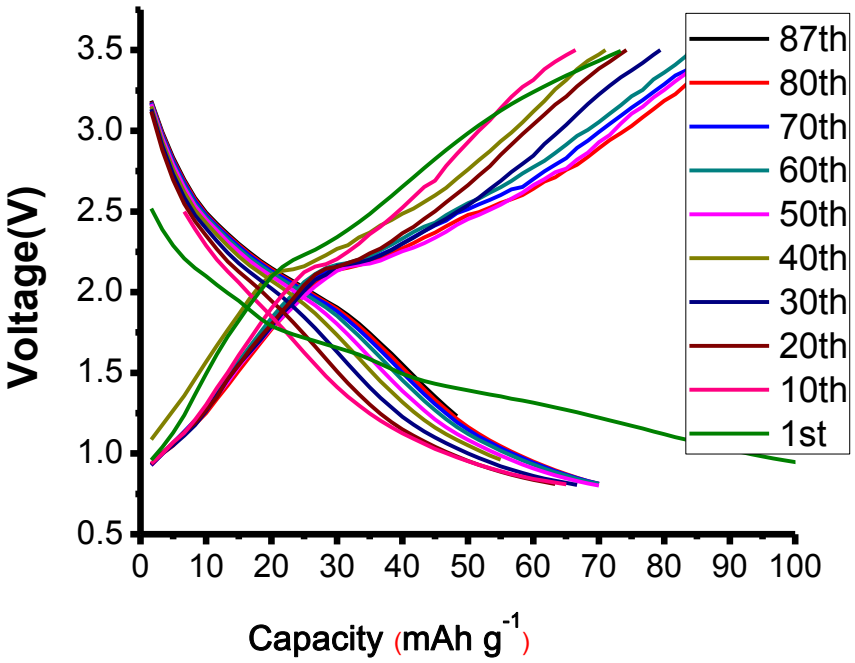

Fig. 13b- Galvanostatic discharging-charging profiles of the Se@MWCNTs cathode at C/6.75 rate

In Fig- 13a and 13b, the initial discharge graph of capacity vs voltage displayed two slope voltage plateaus: initially a short one at 1.75 V and followed by a longer one at 1.1 V, which deal with the multiple phase change reactions at the time of discharge. After the first cycle, the voltages of discharge plateau increased and two new plateaus at 2.5 V and 2 V appeared, which are probably due to the structure change of Se after the first activation process[18]. From the capacity vs cycle number pot, the initial discharge capacity was 140 mAh gm^{-1} and it drops to 70 mAh gm^{-1} within 10 cycles. Thereafter, the charge/discharge capacity is quite stable. These results suggest that the utilization of active Se in the Se@MWCNTs composite film is considerably improved from commercial Selenium due to the conductive three dimensional network structure constructed by MWCNTs. The distribution of Se on MWCNTs surface

significantly improves the electrical conductivity of electrode and Se@MWCNTs composite produces many open channels for Li ion transfer and confinement of polyselenides. The three dimensional structure could effectively accommodate the volume expansion at time of cycling and consequently leading to the long-term stability of Se electrode, but only cycling stability is not enough so a composite of Se@GO by ball milling of selenium and GO was prepared and analyzed. The FE-SEM image of Se@GO is shown below.

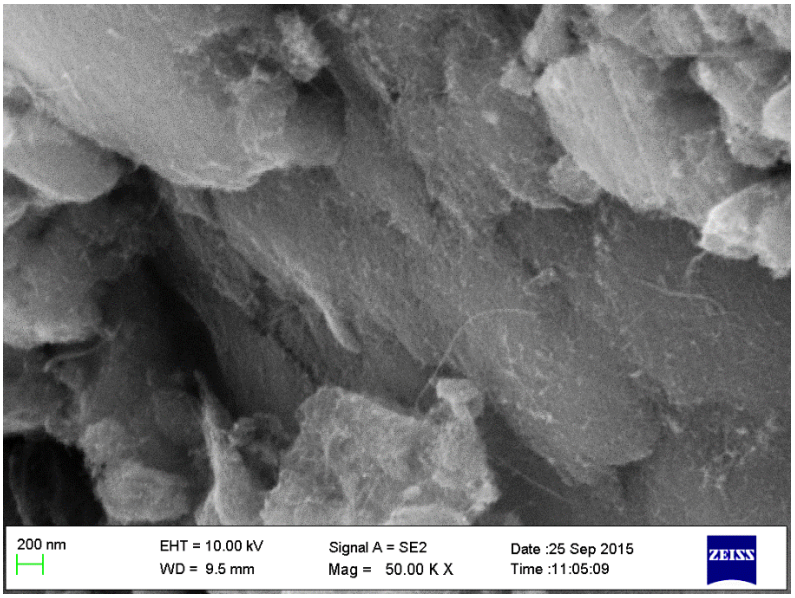

Fig. 14a- FE-SEM image of Se@GO.

In the SEM image it is clearly seen that the selenium and graphene oxide are mixed well, as Se nanoparticles appear to be attached to the GO sheets uniformly. To measure the electrochemical performance, at the current rate C/6.75 and voltage range was 0.8 V to 3.5 V. For this case, the OCV was 3.06 V. The electrochemical behavior is shown in the following figure.

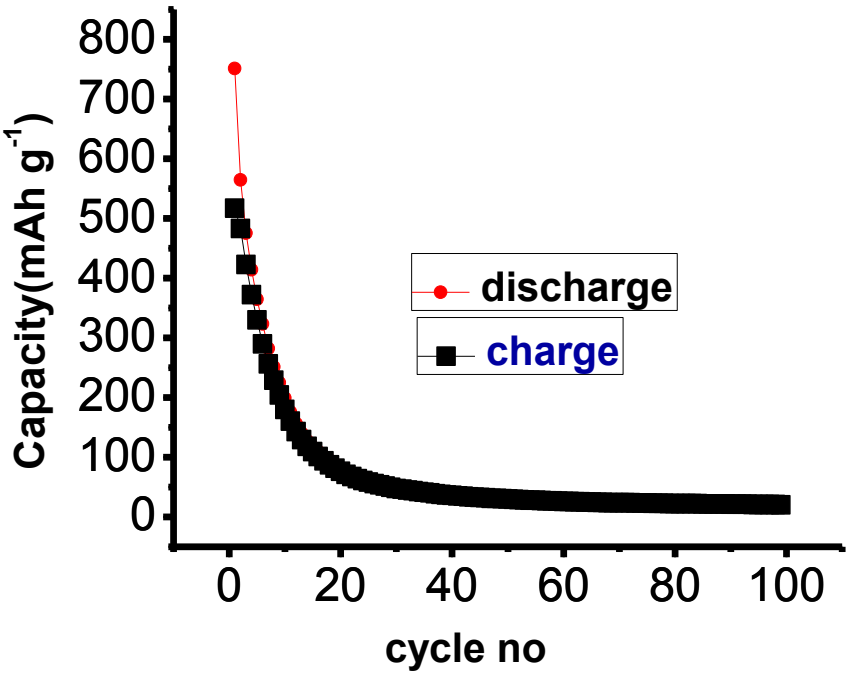

Fig. 15a- Charge-discharge capacity retention plot of the Se@GO cathode.

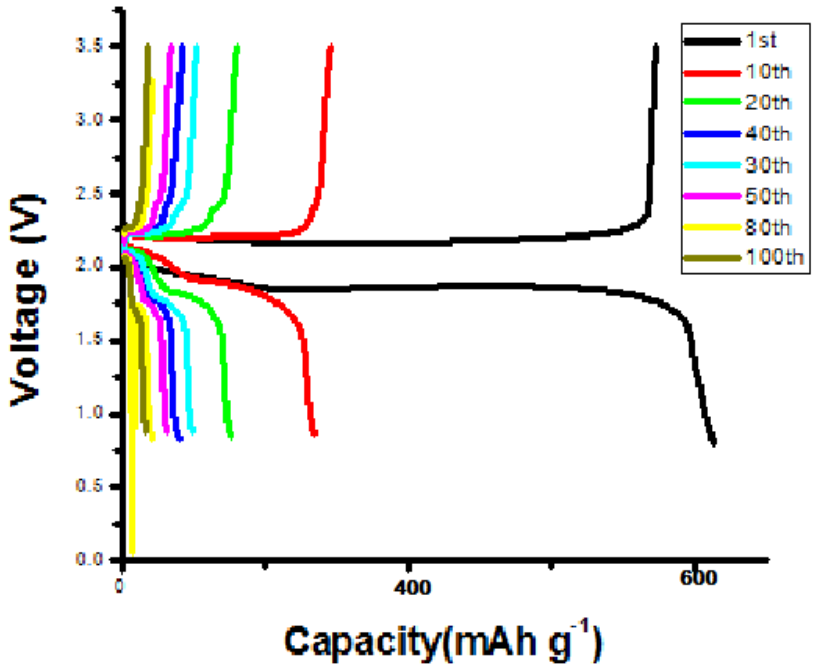

Fig. 15b - Galvano static discharging-charging profiles of the Se@GO cathodes at C/6.75 rate

At the first cycle, the capacity was observed to be more than the theoretical capacity, because of some side-reactions between lithium selenide and electrolyte solutions[19]. In the voltage vs capacity plot for the first cycle, reduction occurs in two voltage plateaus, first at 2 V and second one at 1.8 V, signify the reduction of Se to Li_2Se_x and Li_2Se. After first cycle, the voltage of first reduction increases to 2.2 V due to structural change of Selenium. In the Fig- 15a and 15b the discharge and charge plots, upto the 30 cycles, the capacity is rapidly fading, but after 30 cycles, the cycling stability is extremely good. For this, the explanation is like this- the capacity fading in Lithium selenium battery occurs due to the polyselenides formed during discharge, which are soluble in the electrolyte solution. Up-to 30 cycles, some percentage of the polyselenides formed, will dissolve in the solution and a stage is reached, when the electrolyte solution is saturated. After the formation of the saturated solution, the newly formed polyselenides cannot dissolve in the solution, it is compelled to react. Thereafter, capacity fading does not occur, and cycling stability becomes good. So to prevent fading of capacity by dissolution our main aim should be to inhibit the dissolution of Lithium polyselenides. Futher, if the internal resistance of the cell is reduced, then battery life is expected to improve, so by using these two concepts, selenium nanoparticles embedded in Reduced graphene oxide (RGO) based composites were prepared. RGO has more unsaturation than graphene oxide, and therefore, it is more conductive than GO. When SeO_2 is dissolved in water, then H_2SeO_4 (Selenic acid) is formed. Here if we add $N_2H_4.H_2O$ (Hydrazine.hydrate) it will reduce the Selenic acid to elemental selenium. As Hydrazine is a reducing agent, it will reduce the Graphene oxide to Reduced Graphene oxide. At this stage, hydrothermal treatment with high pressure and certain temperature will convert the elemental Selenium to Selenium nanoparticles. The reaction scheme is shown here.

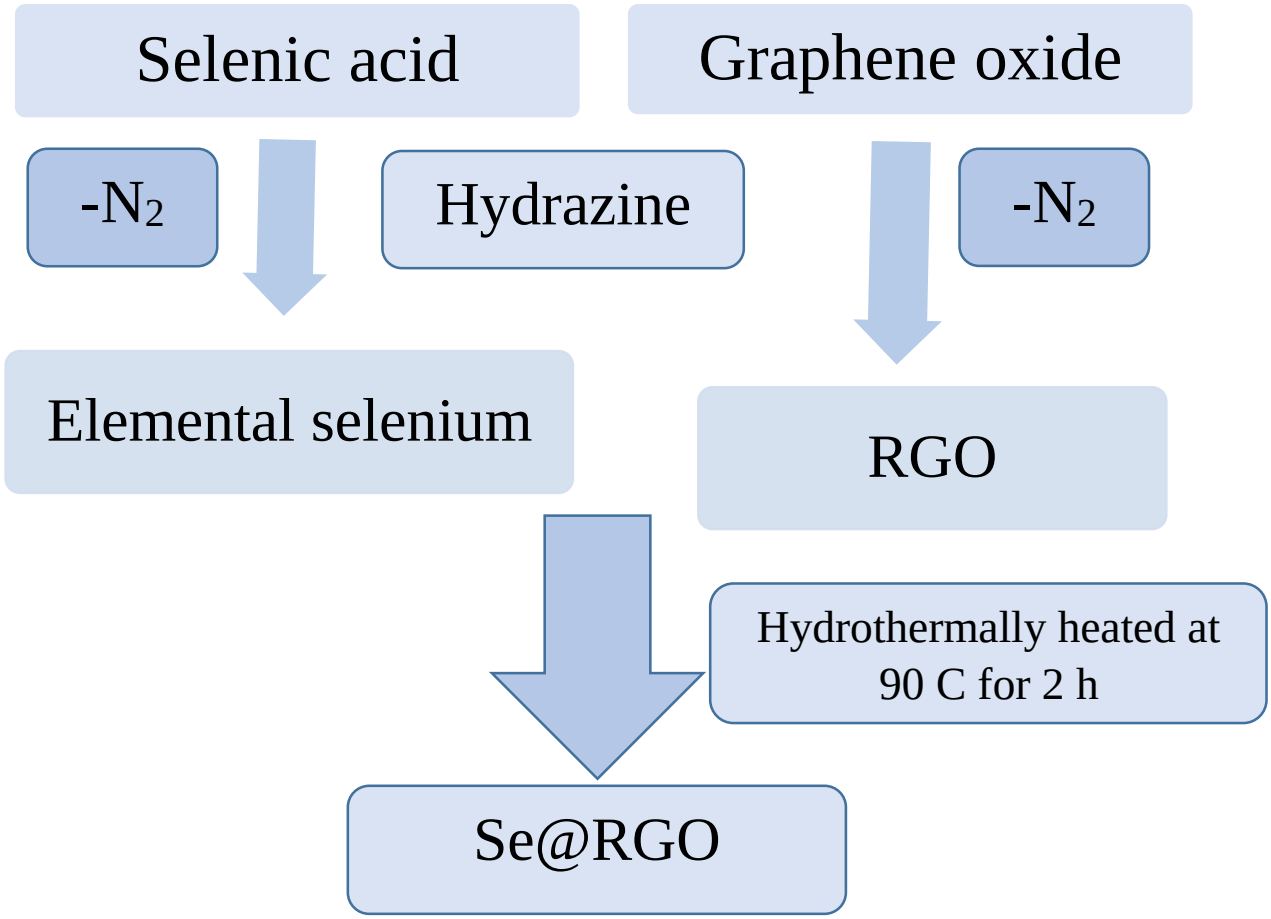

Fig. 20- Schematic for preparing Se@RGO by a hydrothermal method

Using hydrazine, the hydrothermal reduction route is more environmentally friendly compared to the chemical reduction processes[20]. Fig.-21 describes preparation of Selenium nanoparticles and Se@RGO composite. The SEM image of the composite reveals a particulate morphology with aggregated flaky particles which are probably RGO, and it is difficult to distinguish Se from RGO particles. The crystal structures were examined by XRD. As shown in Fig 21, all the peaks are indexed to hexagonal Se (JCPDS 06-0362), indicating that pure Se is formed in the composite and in the nanoparticles.

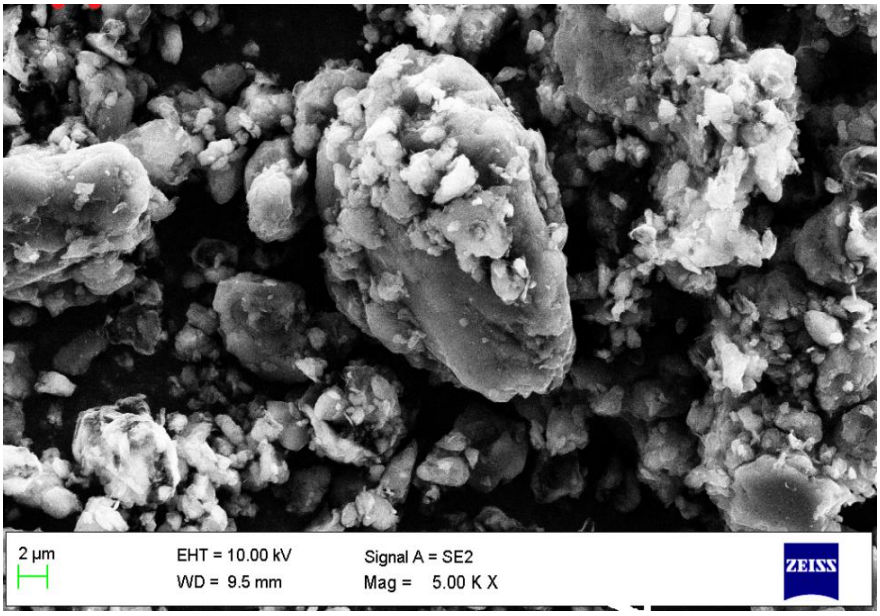

Fig. 21- SEM image of Se@RGO composite

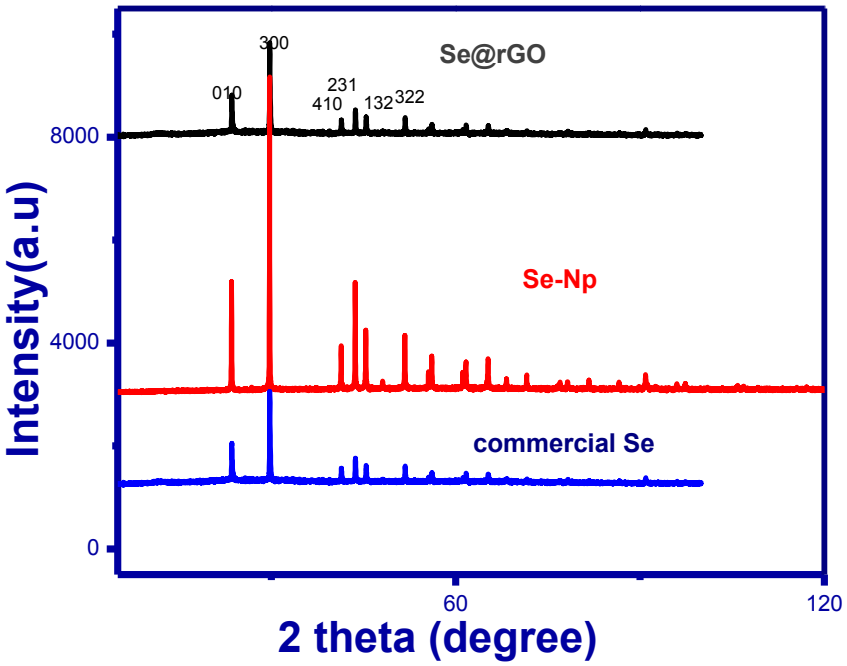

Fig.21- XRD patterns of the commercial selenium, Se NPs and Se@RGO composite.

The cycling performance is further evaluated by galvanostatic charging-discharging tests.

The graphs are shown below.

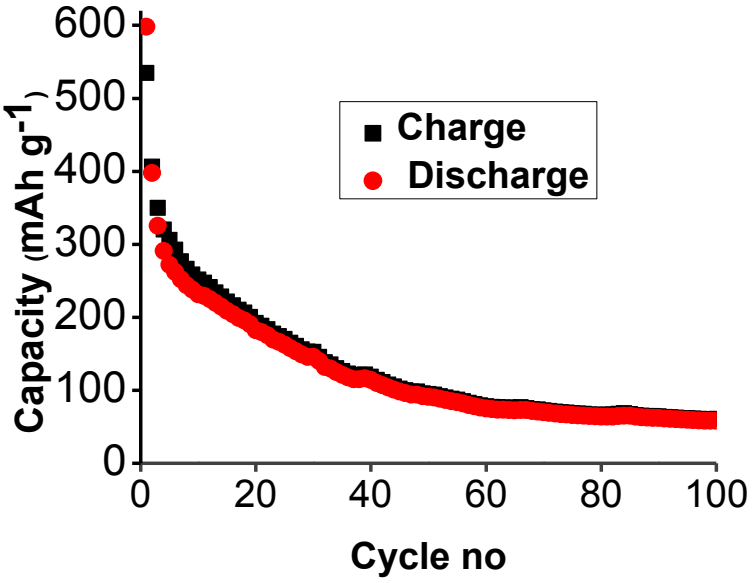

Fig. 22a- Charge discharge capacity retention plot of a Se@RGO cathode.

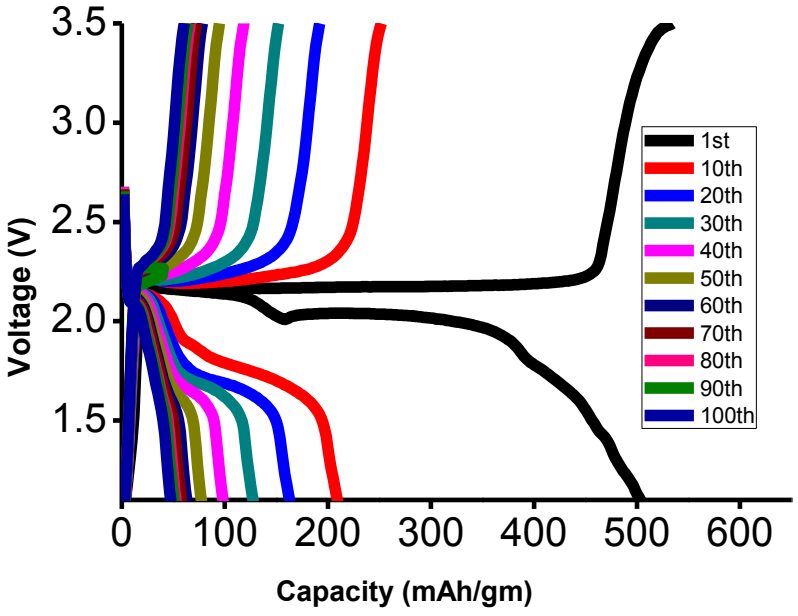

Fig- 22b Galvanostatic discharging-charging profiles of the Se@GO cathodes at C/6.75 rate.

In the voltage vs capacity plot, during reduction, two voltage plateaus are observed, the first one at 2 V and the second one at 1.8 V, which signify the reduction of Se to Li_2Se_x and Li_2Se. The initial discharge capacity was nearly 500 mAh g^{-1}, and at the end the capacity was 110 mAh g^{-1}. There is no rapid capacity fading like previous materials. The Se nanoparticles shorten the transfer path of lithium ions which enhances the rate capability of the cathode. The RGO flakes in Se@RGO can accommodate the stress and volume changes of Se during lithiation/delithiation processes and stop shuttle effect by a robust three dimensional structure, and as a result, better cycling performance than previous cathode materials was achieved.

Conclusions

Four types of Se based active materials, namely, Commercial Se/Carbon black, Se@MWCNTs, Se@GO and Se@RGO composites were synthesized, characterized and electrochemical measurements were done for the corresponding Li-Se cells. Capacity fading was observed for all the materials upto 30 cycles approximately, due to loss of active mass by the formation of dissolvable polyselenides. Among the materials, Se@MWCNTs has a moderately good cycling stability but low capacity and the Se@GO composite cathode has high specific capacity but not good cycling stability, but the in-situ formed Se@RGO composite via a hydrothermal route gave the best electrochemical performance, it has reasonably high capacity and good cycling stability. In future, we plan to initially dissolve polyselenides in the electrolyte solution, so that the newly formed polyselenides will not dissolve in the saturated solution, and marked improvements in capacity and cyclability can be realized..

References

1. C.Uhuegbu, J.Emerg. Trends Eng. Appl. Sci. 2 (2011) 96.
2. S.Whitingham,Chem. Rev. 104 (2014) 4271.
3. A.R.Kamali and D.J.Fray, J. New Mater.Electrochem. Syst.13 (2010) 147.
4. D.Guyomard and J. M. Tarascon, J. Electrochem. Soc. 139 (1992) 937.
5. J. M.Tarascon, W. R. McKinnon, F. Coowar, T. N. Bowner, G. Amatucci and D. Guyomard, J. Electrochem. Soc 141 (1994) 1421.
6. K. Xu, Chem. Rev 104 (2004) 4303
7. Dahl, C.; Prange, A.; Steudel, R. Metabolism of Natural Polymeric Sulfur Compounds. Biopolymers Online; Wiley-VCH: Weinheim, Germany, 2005
8. Mikhaylik, Y.V.216 th Electrochemical Society Meeting Presentation, Vienna, Austria, Oct 4-9, 2010.
9. Rauh, R. D.; Abraham, K. M.; Pearson, G. F.; Surprenant, ,J. K.; Brummer, S. B. J. Electrochem Soc 126 (1979) 523.
10. Mikhaylik, Y. V. Methods of Charging Lithium Sulfur Cells. U.S. Patent 7, 646, 171, Jan 12, 2010.
11. . J. Am. Chem. Soc.134 (2012) 4505−4508
12. W.S. Hummers Jr, R.E. Offeman, Preparation of graphitic oxide, J. Am. Chem. Soc. 80 (1958), 1339-1339.
13. H.A. Becerril, J. Mao, Z. Liu, R.M. Stoltenberg, Z. Bao, Y. Chen, Evaluation of solution-processed reduced graphene oxide films as transparent conductors, ACS Nano 2 (2008) 463-470.
14. J. Power Sources 288 (2015) 214-220

15. H. Qu, Z.A. Zhang, S.F. Jiang, X.W. Wang, Y.Q. Lai, Y.X. Liu, J. Li, Confining selenium in nitrogen-containing hierarchical porous carbon for high-rate rechargeable lithium-selenium batteries, J. Mater. Chem. A 2 (2014), 12255-12261.
16. Y. Cui, A. Abouimrane, J. Lu, T. Bolin, Y. Ren, W. Weng, C. Sun, V. Maroni, S. Heald, K. Amine, J. Am. Chem. Soc. 135 (2013) 8047.
17. S.F. Jiang, Z.A. Zhang, Y.Q. Lai, Y.H. Qu, X.W. Wang, J. Li, J. Power Sources 267 (2014) 394.
18. Y.X. Yin, S. Xin, Y.G. Guo, L.J. Wan, Angew. Chem. Int. Ed. 52 (2013) 2.
19. C. Luo, J.J. Wang, L.M. Suo, J.F. Mao, X.L. Fan, C.S. Wang, J.Mater. Chem. A 3 (2015) 555.